Effect of Sting Oscillations on the Measurement of Dynamic Stability Derivatives

Glen E. Burt* and James C. Uselton†
ARO, Inc. Arnold Air Force Station, Tenn.

Long, slender stings required to minimize support interference on dynamic stability test mechanisms are subject to oscillatory bending because of aerodynamic (particularly for aircraft configurations), structural, and inertial loads. Sting oscillations can cause large errors in dynamic stability measurements using typical data reduction techniques for both forced and free oscillation. In this paper, data reduction equations are derived from equations of motion which include the sting movement. This movement can be measured by instrumentation or calculated from static data. Bench tests and wind tunnel tests using AGARD models B and C verify that accurate data are obtained when the correct data reduction is used.

Nomenclature

A = reference area, model wing planform area 0.974 ft^2
b = reference length for lateral coefficients, wing span 1.50 ft
C_m = pitching-moment coefficient, pitching moment/$q_\infty Ac$
C_n = yawing-moment coefficient, yawing moment/$q_\infty Ab$
C_{m_q} = pitching-moment coefficient due to pitch velocity, $\partial(C_m)/\partial(qc/2V_\infty)$, rad^{-1}
$C_{m_{\dot\alpha}}$ = pitching-moment coefficient due to rate of change of angle of attack, $\partial(C_m)/\partial(\dot\alpha c/2V_\infty)$, rad^{-1}
C_{m_α} = pitching-moment coefficient due to angle of attack, $\partial(C_m)/\partial\alpha$, rad^{-1}
C_{n_r} = yawing-moment coefficient due to yaw velocity, $\partial(C_n)/\partial/rb/2V_\infty)$, rad^{-1}
C_{n_β} = yawing-moment coefficient due to slideslip angle, $\partial(C_n)/\partial\beta$, rad^{-1}
$C_{n_{\dot\beta}}$ = yawing-moment coefficient due to rate of change of slideslip angle, $\partial(C_n)/\partial(\dot\beta b/2V_\infty)$
c = reference length for longitudinal coefficients, wing mean aerodynamic chord 0.866 ft
F_{N_α} = slope of the normal force vs α curve, lb/rad
F_p = force applied to the sting at the pivot axis, lb
I_y = model moment of inertia about the cross-flexure pivot axis (y body axis), slug-ft^2
K_l = moment-beam strain-gage-bridge calibration constant, ft-lb/volt
K_o = cross-flexure strain-gage-bridge calibration constant, rad/volt
K_s = sting strain-gage-bridge calibration constant, ft-lb/volt
M = aerodynamic pitching moment, ft-lb
M_b = moment applied by the balance to oscillate the model, ft-lb
M_p = moment applied to the sting at the cross-flexure pivot, ft-lb
M_s = moment applied to the sting as measured by the sting strain-gage bridge, ft-lb
M_q = pitching moment due to pitch velocity, $\partial M/\partial q$, ft-lb-sec/rad
M_α = pitching moment due to angle of attack, $\partial M/\partial\alpha$, ft-lb/rad
$M_{\dot\alpha}$ = pitching moment due to rate of change of angle of attack, $\partial M/\partial\dot\alpha$, ft-lb-sec/rad
M_{θ_f} = cross-flexure stiffness (with no static force loads unless otherwise specified), ft-lb/rad
δM_{θ_f} = M_{θ_f} (under load) − M_{θ_f} (no load), ft-lb/rad
$M_{\dot\theta_f}$ = cross-flexure damping moment, ft-lb-sec/rad
M_∞ = freestream Mach number
q = pitching velocity, rads/sec
q_∞ = tunnel freestream dynamic pressure, lb/ft^2
r = yawing velocity, rad/sec
t = time, sec
V_∞ = tunnel freestream velocity, fps
W = model mass, slugs
W_e = effective model and sting mass at the pivot axis, slugs
x_{cg} = location of model center of gravity with respect to the pivot axis, ft
x_p = location of the pivot axis with respect to the model nose, ft or in.
z = translation of the pivot axis normal to the sting (Fig. 1), ft
α = angle of attack measured from the reference condition, α_M, rads
α_M = mean angle of attack, deg
β = sideslip angle, rads
Γ = phase angle between sting oscillation angle, θ_s, and flexure oscillation angle, θ_f (positive when θ_s leads), rads or deg
γ = phase angle between input moment, M_b, and flexure oscillation angle, θ_f (positive when M_b leads), rads or deg
η = phase angle in solution to free-oscillation equation of motion, rads
θ = angular displacement in pitch, rads
$\bar\theta_0$ = angular displacement amplitude at time equal zero, rads
λ = damping exponent in solution to free-oscillation equation of motion, sec^{-1}
ω = model angular oscillation frequency, rads/sec
ω_{n_f} = model-flexure undamped natural frequency (sting rigid)$(-M_{\theta_f}/I_y)^{1/2}$, rads/sec
ω_s = natural frequency of the model-sting system, rads/sec
$\dot{(\ )}$, $\ddot{(\ )}$ = first and second derivatives with respect to time, t
$\bar{(\ )}$ = amplitude

Subscripts

f = cross flexure

Presented as Paper 74-612 at the AIAA 8th Aerodynamic Testing Conference, Bethesda, Md., July 8-10, 1974; submitted Aug. 1, 1974; revision received June 13, 1975. The research reported here was conducted by the Arnold Engineering Development Center, Air Force Systems Command. Research results were obtained by personnel of ARO, Inc., contract operator at AEDC. Further reproduction is authorized to satisfy needs of the U.S. Government.

*Supervisor, Dynamics Group, Aerodynamics Projects Branch, von Karman Gas Dynamics Facility (VKF). Member AIAA.

†Supervisor, Impulse Tunnels and Dynamics Section, Aerodynamics Projects Branch, VKF. Associate Fellow AIAA.

m = model
mag = magnetic damper
S = static component
s = sting

I. Introduction

DURING the development of a forced-oscillation test mechanism for measuring the damping in pitch or yaw of lifting vehicles,[1] it was found that sting bending effects could strongly influence the measurements. The slender sting required for testing airplane configurations, coupled with the large lift forces of such configurations, created relatively large amplitude sting oscillations. The present trend to use extremely long, slender stings on dynamic stability test mechanisms to minimize support interference has introduced significant sting oscillations even for re-entry vehicle (R/V) configurations. The effects of the sting oscillations on the measurements are two-fold: first, the moments created by the plunging motion are not normally included in the equations of motion used for data reduction; and secondly, the model angular position is not correctly measured because of the sting angular deflection.

In this paper the data reduction equations are derived from equations of motion including the sting oscillations for both forced- and free-oscillation test techniques. It is shown that the data reduction equations are not very difficult if the natural sting frequency is not too close to the model oscillation frequency. The sting oscillations required in the data reduction equations can be measured by intrumenting the sting with strain gages, or can be calculated from the sting equations of motion using known or estimated static stability data. The validity of this data reduction procedure is proven using the forced-oscillation technique. Bench tests using a magnetic damper and wind tunnel tests using AGARD Calibration Models B and C were conducted, and the results indicate that accurate data can be obtained if the data are corrected for sting oscillations.

II. Data Reduction Equations

A. General

Figure 1 is a schematic of a model oscillating in pitch about the cross-flexure pivot, and translating normal to the sting. The oscillation angle typically measured is the rotation across the cross-flexure θ_f, which is obtained from strain gages on the flexures.[2] It should be noted that as the mechanism is pitched, static forces and moments are applied which deflect the sting and flexures. These static deflections affect only the mean angle of attack α_M, and for clarity are not shown. It is apparent from Fig. 1 that the model oscillatory angle of attack can be written as

$$\alpha=\theta_m+\frac{\dot{z}}{V_\infty\cos\alpha_M} \tag{1}$$

and the angular rotation θ_m, is composed of two deflections

$$\theta_m=\theta_f+\theta_s \tag{2}$$

The moment equation of motion of the model written in body axis about the cross-flexure pivot, and allowing for model unbalance (normally models are balanced before testing, but some slender configurations cannot be accurately balanced), is

$$I_y\ddot{\theta}_m-Wx_{cg}\ddot{z}-M_q\dot{\theta}_m-M_{\dot\alpha}\dot\alpha-M_{\dot\theta_f}\dot\theta_f$$
$$-M_\alpha\alpha-(M_{\theta_f}+\delta M_{\theta_f})\theta_f=M_b \tag{3}$$

The term δM_{θ_f} is included because the flexure stiffness varies with axial and normal force.[3] δM_{θ_f} is determined in the data reduction from known or estimated force data. Bench tests have shown that $M_{\dot\theta_f}$ is essentially unaffected by static loads. M_b is the forcing moment applied when using the forced-oscillation technique, and is zero for the free-oscillation case. Substituting Eqs. (1) and (2) into Eq. (3), one obtains the following equation of motion

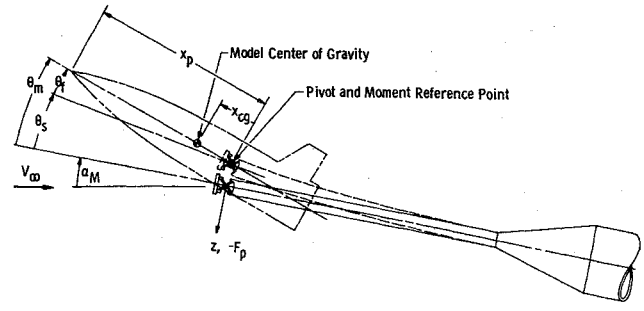

Fig. 1 Schematic illustrating model and sting oscillatory motion.

$$I_y(\ddot\theta_f+\ddot\theta_s)-Wx_{cg}\ddot z-M_q(\dot\theta_f+\dot\theta_s)$$
$$-M_{\dot\alpha}\left(\dot\theta_f+\dot\theta_s+\frac{\ddot z}{V_\infty\cos\alpha_M}\right)-M_{\dot\theta_f}\dot\theta_f$$
$$-M_\alpha\left(\theta_f+\theta_s+\frac{\dot z}{V_\infty\cos\alpha_M}\right)$$
$$-(M_{\theta_f}+\delta M_{\theta_f})\theta_f=M_b \tag{4}$$

B. Forced Oscillation

The solution of Eq. (4) for a model undergoing a steady-state oscillation at an amplitude $\bar\theta_m$ and frequency ω is

$$\theta_f=\bar\theta_f\cos(\omega t)$$
$$\theta_s=\bar\theta_s\cos(\omega t+\Gamma)=\bar\theta_s[\cos(\omega t)\cos\Gamma-\sin(\omega t)\times\sin\Gamma]$$
$$z=-\bar z\cos(\omega t+\Gamma)=-\bar z[\cos(\omega t)\cos\Gamma-\sin(\omega t)\times\sin\Gamma]$$
$$M_b=\bar M_b\cos(\omega t+\gamma)=\bar M_b[\cos(\omega t)\cos\gamma-\sin(\omega t)\sin\gamma] \tag{5}$$

If the frequency of oscillation is not near the natural frequency of the sting ($\omega_s>1.5\,\omega$), and the system is rigidly mounted, the phase angle Γ will be near zero or 180°, depending on the variation of normal force with θ_m. Substituting Eq. (5), with $\sin\Gamma=0$, into Eq. (4), and solving for the aerodynamic moments gives

$$M_q+M_{\dot\alpha}=\left(-\frac{\bar M_b}{\omega\bar\theta_f}\sin\gamma+\frac{M_\alpha}{V_\infty\cos\alpha_M}\frac{\bar z\cos\Gamma}{\bar\theta_f}-M_{\dot\theta_f}\right)\Big/\left(1+\frac{\bar\theta_s\cos\Gamma}{\bar\theta_f}\right) \tag{6}$$

$$M_\alpha=M_{\theta_f}\left[\left(\frac{\omega}{\omega_{n_f}}\right)^2-1\right]+\left(M_{\theta_f}\frac{\bar\theta_s\cos\Gamma}{\bar\theta_f}-\delta M_{\theta_f}-\frac{\bar M_b}{\bar\theta_f}\cos\gamma-Wx_{cg}\omega^2\frac{\bar z\cos\Gamma}{\bar\theta_f}\right)\Big/\left(1+\frac{\bar\theta_s\cos\Gamma}{\bar\theta_f}\right) \tag{7}$$

where $-M_{\theta_f}/\omega_{n_f}{}^2$ has been substituted for I_y, and the term

$$\frac{\bar z\cos\Gamma}{\bar\theta_f}\quad\frac{M_{\dot\alpha}\omega^2}{V_\infty\cos\alpha_M}$$

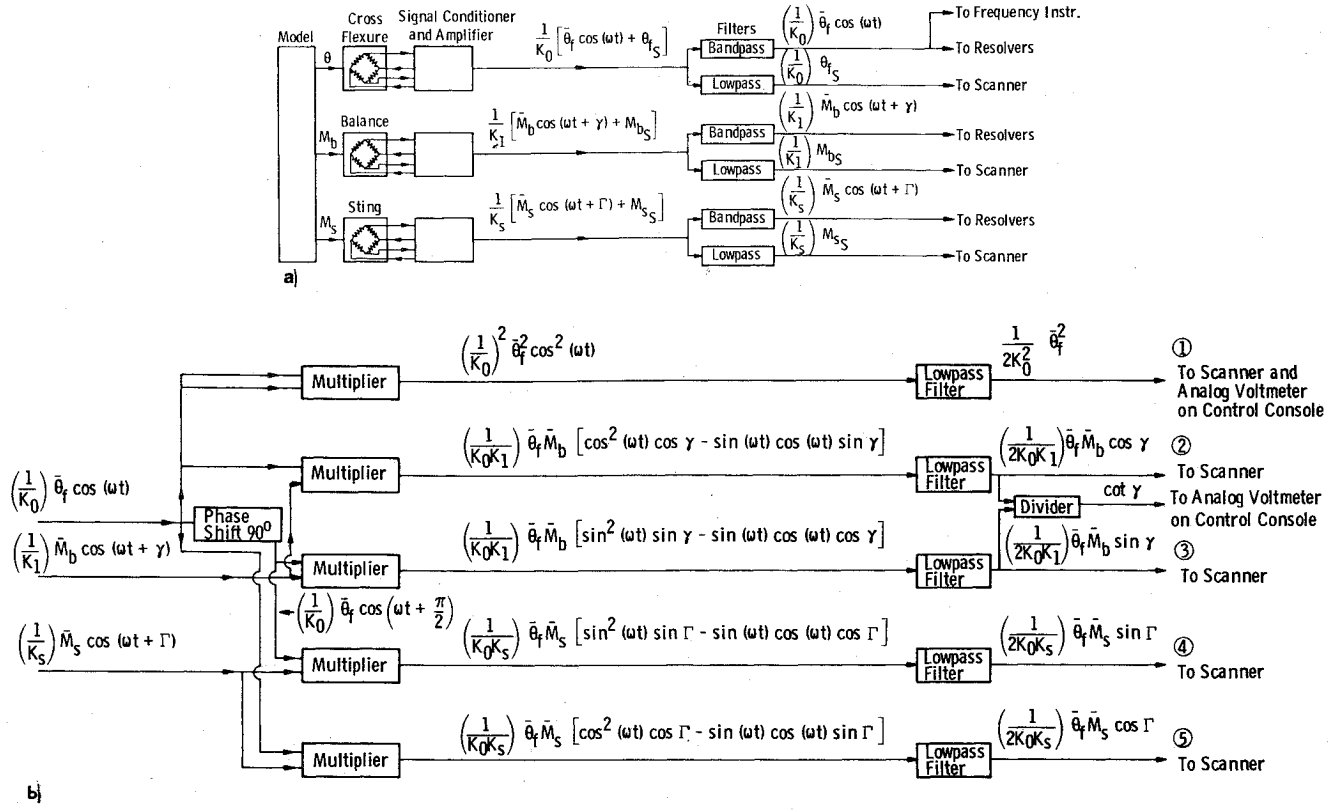

Fig. 2 Data acquisition instrumentation schematic. a) Basic outputs. b) Resolver system.

that occurs in Eq. (7) is small and has been neglected.

C. Free Oscillation

Using the same assumptions about sting frequency and mounting as in the forced-oscillation case, the forces and moments that cause the sting oscillations are primarily functions of θ_f. Therefore θ_s and z are essentially linearly dependent on θ_f, and the following relations can be written

$$\frac{\theta_s}{\theta_f}=\frac{\dot\theta_s}{\dot\theta_f}=\frac{\ddot\theta_s}{\ddot\theta_f}=\frac{\bar\theta_s}{\bar\theta_f}\cos\Gamma \tag{8a}$$

$$\frac{z}{\theta_f}=\frac{\dot z}{\dot\theta_f}=\frac{\ddot z}{\ddot\theta_f}=-\frac{\bar z}{\bar\theta_f}\cos\Gamma \tag{8b}$$

Since the sting is not oscillating near its natural frequency, its structural damping is sufficient to damp its motion, such that the above relations apply even when the model amplitude is changing. Substituting Eqs. (8) into Eq. (4), with $M_b=0$, one obtains the following equation which contains only one time dependent variable, θ_f:

$$\left[I_y\left(1+\frac{\bar\theta_s}{\bar\theta_f}\cos\Gamma\right)+Wx_{cg}\left(\frac{\bar z}{\bar\theta_f}\cos\Gamma\right)\right]\ddot\theta_f$$
$$-\left[\left(M_q+M_{\dot\alpha}\right)\left(1+\frac{\bar\theta_s}{\bar\theta_f}\cos\Gamma\right)+M_{\dot\theta_f}-\frac{M_\alpha}{V_\infty\cos\alpha_M}\left(\frac{\bar z}{\bar\theta_f}\cos\Gamma\right)\right]\dot\theta_f$$
$$-\left[M_\alpha\left(1+\frac{\bar\theta_s}{\bar\theta_f}\cos\Gamma\right)+\left(M_{\theta_f}+\delta M_{\theta_f}\right)\right]\theta_f=0 \tag{9}$$

where again the term

$$\frac{\bar z\cos\Gamma}{\bar\theta_f}\quad\frac{M_{\dot\alpha}\omega^2}{V_\infty\cos\alpha_M}$$

is small and has been neglected. The solution is

$$\theta_f=\bar\theta_o e^{\lambda t}\cos\left(\omega t+\eta\right) \tag{10}$$

where

$$\lambda=\left[\left(M_q+M_{\dot\alpha}\right)\left(1+\frac{\bar\theta_s}{\bar\theta_f}\cos\Gamma\right)+M_{\dot\theta_f}-\frac{M_\alpha}{V_\infty\cos\alpha_M}\left(\frac{\bar z}{\bar\theta_f}\cos\Gamma\right)\right]/2\left[I_y\left(1+\frac{\bar\theta_s}{\bar\theta_f}\cos\Gamma\right)+Wx_{cg}\left(\frac{\bar z}{\bar\theta_f}\cos\Gamma\right)\right]$$

$$\omega\left[1+\left(\frac{\lambda}{\omega}\right)^2\right]^{1/2}=-\left\{\left[M_\alpha\left(1+\frac{\bar\theta_s}{\bar\theta_f}\cos\Gamma\right)+\left(M_{\theta_f}+\delta M_{\theta_f}\right)\right]/\left[I_y\left(1+\frac{\bar\theta_s}{\bar\theta_f}\cos\Gamma\right)+Wx_{cg}\left(\frac{\bar z}{\bar\theta_f}\cos\Gamma\right)\right]\right\}^{1/2}$$

Using the log decrement technique and assuming $(\lambda/\omega)^2$ is negligible, the aerodynamic moments can be written as follows

$$M_q+M_{\dot\alpha}=2\left(\frac{-M_{\theta_f}}{\omega_{\eta f}^{\,2}}\right)\frac{d(\ell n\bar\theta_f)}{dt}\left[1-\frac{Wx_{cg}\left(\frac{\bar z}{\bar\theta_f}\cos\Gamma\right)\omega_{\eta f}^{\,2}}{M_{\theta_f}\left(1+\frac{\bar\theta_s}{\bar\theta_f}\cos\Gamma\right)}\right]$$
$$-\frac{M_\alpha}{1+\frac{\bar\theta_s}{\bar\theta_f}\cos\Gamma}+\left(\frac{M_\alpha}{V_\infty\cos\alpha_M}\right)\left(\frac{\frac{\bar z}{\bar\theta_f}\cos\Gamma}{1+\frac{\bar\theta_s}{\bar\theta_f}\cos\Gamma}\right) \tag{11}$$

$$M_\alpha=M_{\theta_f}\left[\left(\frac{\omega}{\omega_{\eta f}}\right)^2-1\right]-\frac{Wx_{cg}(\omega^2)\left(\frac{\bar z}{\bar\theta_f}\cos\Gamma\right)}{1+\frac{\bar\theta_s}{\bar\theta_f}\cos\Gamma}$$
$$+M_{\theta_f}\left[\frac{\frac{\bar\theta_s}{\bar\theta_f}\cos\Gamma}{1+\frac{\bar\theta_s}{\bar\theta_f}\cos\Gamma}\right]-\frac{\delta M_{\theta_f}}{1+\frac{\bar\theta_s}{\bar\theta_f}\cos\Gamma} \tag{12}$$

D. Determination of Sting Oscillation

The most accurate method of determining the sting oscillation is to instrument the sting with a strain-gage bridge and measure the dynamic moment (details of this measurement are in Sec. IIIA). The dynamic moment at the flexure pivot is known from the flexure stiffness M_{θ_f}, and the oscillation angle θ_f. Thus, the sting oscillation can be determined from these two moments and the sting deflection constants as follows

$$\frac{\bar{z}\cos\Gamma}{\bar{\theta}_f} = M_{\theta_f}\left(\frac{\partial z}{\partial M_p}\right)_{M_s} - \left(\frac{\bar{M}_s\cos\Gamma}{\bar{\theta}_f}\right)\left(\frac{\partial z}{\partial M_s}\right)_{M_p} \tag{13}$$

$$\frac{\bar{\theta}_s\cos\Gamma}{\bar{\theta}_f} = -M_{\theta_f}\left(\frac{\partial \theta_s}{\partial M_p}\right)_{M_s} + \left(\frac{\bar{M}_s\cos\Gamma}{\bar{\theta}_f}\right)\left(\frac{\partial \theta_s}{\partial M_s}\right)_{M_p} \tag{14}$$

The subscripts on the partial derivatives (deflection constants) indicate the parameter that is held constant.

If the sting is not instrumented and static force data are available, the sting oscillations can be calculated from the dynamic force and moment at the pivot

$$\frac{\bar{z}\cos\Gamma}{\bar{\theta}_f} = M_{\theta_f}\left(\frac{\partial z}{\partial M_p}\right)_{F_p} - \left(\frac{F_p}{\theta_f}\right)\left(\frac{\partial z}{\partial F_p}\right)_{M_p} \tag{15}$$

$$\frac{\bar{\theta}_s\cos\Gamma}{\bar{\theta}_f} = -M_{\theta_f}\left(\frac{\partial \theta_s}{\partial M_p}\right)_{F_p} + \left(\frac{F_p}{\theta_f}\right)\left(\frac{\partial \theta_s}{\partial F_p}\right)_{M_p} \tag{16}$$

The force F_p can be calculated from the force equation of motion

$$F_p = F_{N_\alpha}\theta_m + W_e\ddot{z} - Wx_{cg}\ddot{\theta}_f \tag{17}$$

where the damping has been neglected. Assuming harmonic motion and using Eqs. (2) and (8), one can write Eq. (17)

$$\frac{F_p}{\theta_f} = F_{N_\alpha}\left(1+\frac{\theta_s}{\bar{\theta}_f}\cos\Gamma\right) + W_e\omega^2\frac{\bar{z}}{\bar{\theta}_f}\cos\Gamma + Wx_{cg}\omega^2 \tag{18}$$

Substituting Eq. (18) into Eqs. (15) and (16) gives

$$\frac{\bar{z}\cos\Gamma}{\bar{\theta}_f} = \left\{ M_{\theta_f}\left(\frac{\partial z}{\partial M_p}\right)_{F_p} - F_{N_\alpha}\left(\frac{\partial z}{\partial F_p}\right)_{M_p}\left[\frac{1 - M_{\theta_f}\left(\frac{\partial \theta_s}{\partial M_p}\right)_{F_p} - \left(\frac{\omega}{\omega_s}\right)^2\left(\frac{\partial \theta_s}{\partial F_p}\right)_{M_p}\left(\frac{W}{W_e}\right)(x_{cg})\Big/\left(\frac{\partial z}{\partial F_p}\right)_{M_p}}{1 - F_{N_\alpha}\left(\frac{\partial \theta_s}{\partial F_p}\right)_{M_p}}\right] + \left(\frac{\omega}{\omega_s}\right)^2\left(\frac{W}{W_e}\right)x_{cg}\right\} \Bigg/ \left[1 - \frac{(\omega/\omega_s)^2}{1 - F_{N_\alpha}\left(\frac{\partial \theta_s}{\partial F_p}\right)_{M_p}}\right] \tag{19}$$

$$\frac{\bar{\theta}_s\cos\Gamma}{\bar{\theta}_f} = \frac{-M_{\theta_f}\left(\frac{\partial \theta_s}{\partial M_p}\right)_{F_p} + F_{N_\alpha}\left(\frac{\partial \theta_s}{\partial F_p}\right)_{M_p} - \left(\frac{\omega}{\omega_s}\right)^2\left(\frac{\partial \theta_s}{\partial F_p}\right)_{M_p}\left(\frac{\bar{z}\cos\Gamma}{\bar{\theta}_f} + \left(\frac{W}{W_e}\right)x_{cg}\right)\Big/\left(\frac{\partial z}{\partial F_p}\right)_{M_p}}{1 - F_{N_\alpha}\left(\frac{\partial \theta_s}{\partial F_p}\right)_{M_p}} \tag{20}$$

where

$$\omega_s \equiv \left[-\left(\frac{\partial z}{\partial F_p}\right)_{M_p} W_e\right]^{-1/2}$$

E. Aerodynamic Coefficients

The aerodynamic pitching moments can be expressed in coefficient form as

$$C_{m_q} + C_{m_{\dot{\alpha}}} = \frac{(M_q + M_{\dot{\alpha}})(2V_\infty)}{q_\infty A c^2} \qquad C_{m_\alpha} = M_\alpha / q_\infty A c \tag{21}$$

The preceding analysis has been written for a model oscillating in pitch, but is also applicable to a model oscillating in yaw. The sting oscillations, in the plane of the motion, are usually considerably smaller for a yawing model. For yaw, the pitch coefficients $C_{m_q} + C_{m_{\dot{\alpha}}}$ and C_{m_α}, are replaced by $C_{n_r} - C_{n_{\dot{\beta}}}\cos\alpha_M$ and $-C_{n_\beta}\cos\alpha_M$, respectively, with the appropriate change in reference length.

III. Procedure and Instrumentation

A. Forced-Oscillation Measurements

The forced-oscillation control, monitor, and data acquisition instrumentation are contained in a portable console that can be interfaced with the instrumentation of the various wind tunnels. The control instrumentation provides a system which can vary the oscillation frequency, oscillation amplitude, and position of the model within the flexure and balance limits. An electronic feedback loop is used to control the oscillation amplitude, which permits testing both dynamically stable and unstable configurations.

Data are normally obtained at or near the natural frequency of the model-flexure system; however, electronic resolvers permit data to be obtained off resonance. A schematic of the data acquisition system is shown in Fig. 2. The strain-gage bridges on the flexures, balance, and sting are excited by dc voltages, and outputs are increased to optimum values by dc amplifiers. Typical outputs from an oscillating model are composed of oscillatory components (OC) superimposed on static components (SC). These components are separated in the data system by bandpass and lowpass filters. The SC outputs are sent directly through the tunnel instrument scanner to the computer, which calculates the static pitching moment C_m, and static sting deflections. The OC outputs are put into the resolver instrumentation (Fig. 2b) and precise frequency measuring instrumentation developed at AEDC-VKF. The resolvers process the OC signals and output dc voltages, which are proportional to the amplitude squared, in-phase and quadrature balance moments, and the in-phase and quadrature sting moments. By dividing outputs 2, 3, and 5 (Fig. 2b) by output 1 and applying the appropriate calibration constants, one obtains the terms $\bar{M}_b\cos\gamma/\bar{\theta}_f$, $M_b\sin\gamma/\bar{\theta}_f$, and $\bar{M}_s\cos\Gamma/\bar{\theta}_f$ required in data reduction Eqs. (6, 7, 13, and 14). From outputs 4 and 5 the phase angle Γ can be measured to verify the assumption that it is near 0 or 180°. The frequency instrument controls the length of the data interval in increments from 2 to 60 sec, during which the scanner reads each input approximately 10 times per sec.

B. Free-Oscillation Measurement

The free-oscillation control and data acquisition systems, with the exception of sting oscillations, can be found in Ref. 2. The term $d(\ell n\bar{\theta}_f)/dt$ in Eq. (11) is obtained from the

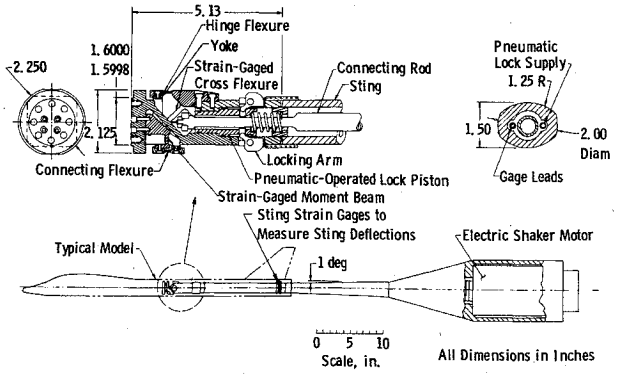

Fig. 3 VKF 1.B test mechanism.

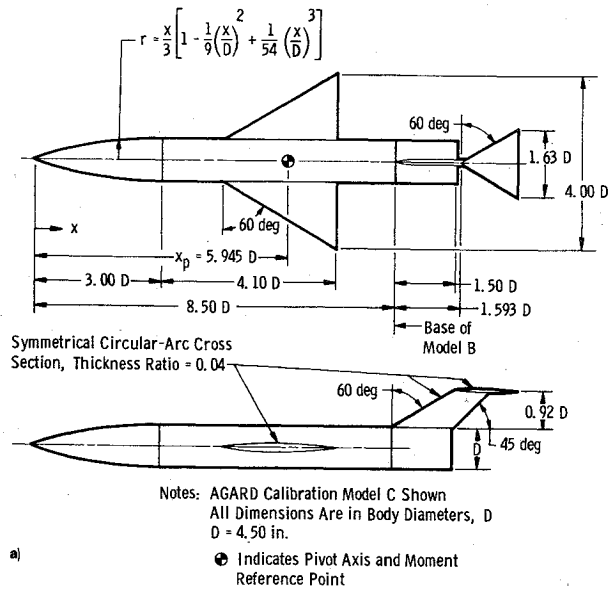

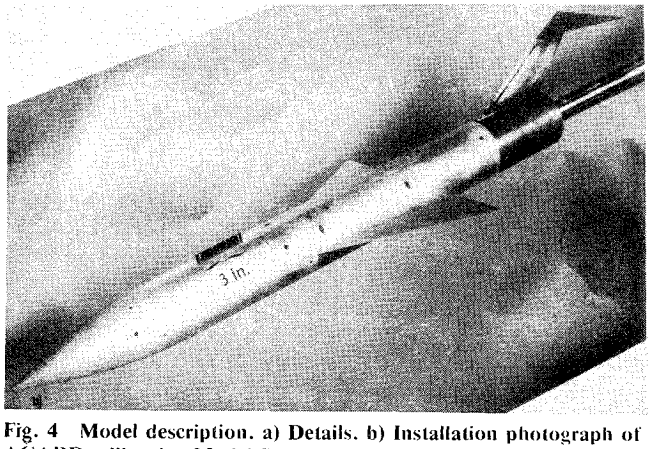

Fig. 4 Model description. a) Details. b) Installation photograph of AGARD calibration Model C.

angular displacement time history. The sting dynamic moment can be measured by using instrumentation that is similar to that used for the forced-oscillation measurements.

C. Calibration and Tare Measurements

The balance and sting calibration constants K_0, K_1, K_s, flexure stiffness $M_{\theta f}$, and sting deflection constants $\partial\theta_s/\partial F_p$, $\partial\theta_s/M_p$, $\partial z/\partial F_p$, $\partial z/\partial M_p$, are determined by applying known loads and measuring the displacements and balance outputs. The sting deflection constants as functions of M_s and M_p, if required, can be calculated from the aforementioned constants. The structural (tare) damping $M_{\theta f}$, is determined from measurements at vacuum conditions similar to those

Sym	Wx_{cg}, slug-ft^2	I_y (actual), slug-ft^2	I_y (calculated), slug-ft^2	ω_{n_f}, rad/sec	Sting
○	0	0.312	0.312	54.85	Rigid
△	0.233	0.328	0.328	53.45	Rigid
■	0.233	0.328	0.379	49.72	Oscillating (Sting Bending Effect Not Included in Data Reduction)
□	0.233	0.328	0.322	53.92	Oscillating (Sting Bending Effect Included in Data Reduction)

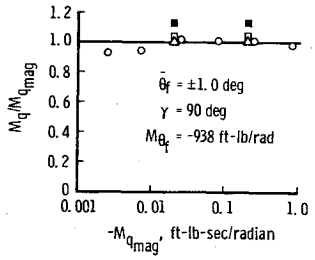

Fig. 5 Comparison of pitch-damping measurement to magnetic damper input.

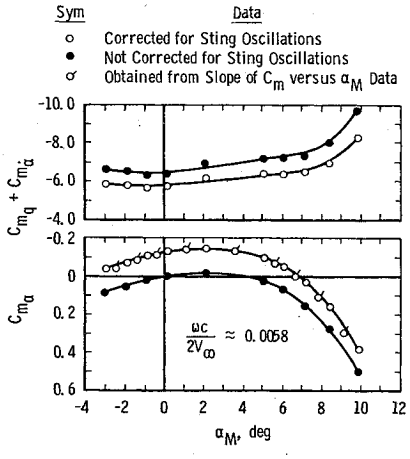

Fig. 6 Effect of sting oscillations on the pitch stability derivatives of Model C at Mach 2.5.

described in Ref. 2. ω_{n_f} is obtained from Eq. (12), using measurements for ω and sting oscillation obtained at vacuum conditions (i.e., $M_\alpha = 0$).

IV. Evaluation Tests and Apparatus

A. Test Description

Bench tests and wind tunnel tests using the forced-oscillation technique were conducted to evaluate the data reduction. The bench tests utilized a two-arm magnetic damper to produce known damping moments. A signal coil, input coil, and feedback loop were used in the damper, which could produce both stable and unstable moments of varying magnitude. The tests were conducted with the test assembly balanced about the pivot axis, and also with a large unbalance. This unbalance caused oscillations of the sting when conventionally supported, but the sting could also be rigidly supported during the bench tests to eliminate the oscillations. The wind tunnel tests were conducted in the AEDC-VKF supersonic Tunnel A at Mach numbers 2.5, 3.0, 3.5, and 4.0, at angles of attack from -5 to 12°, and at a Reynolds number of 4×10^6 based on the wing mean aerodynamic chord c, using the AEDC-VKF 1.B test mechanism.

B. Test Mechanism

The pitch/yaw damping test mechanism shown in Fig. 3 utilizes a cross-flexure pivot, a one-component moment beam, and an electric shaker motor. The motor is coupled to the moment beam by means of a connecting rod and flexural

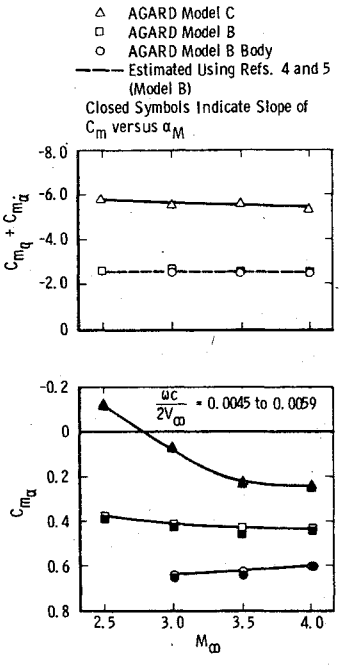

Fig. 7 Variation of the pitch stability derivatives at $\alpha_M = 0$ with Mach number.

linkage which converts the translational force to a moment (70 in.-lb maximum) in order to oscillate the model at amplitudes up to ±2° and frequencies from 2 to 20 Hz. The cross-flexures, which are instrumented to measure the pitch/yaw displacement, support the model loads and provide the restoring moment, to cancel the inertia moment when the system is operating at its natural frequency. The existing cross-flexures are composed of three 0.170 in. thick beams, with single unit construction, and produce a restoring moment of -938 ft-lb/rad. Since the moment beam which is used to measure the forcing moment is not subjected to the static loads, it can be made as sensitive as required for the dynamic measurements. Presently, four beams exist which can measure up to ±3, ±11, ±25 (used for these tests), and ±70 in.-lb. A pneumatic- and spring-operated locking device is provided to hold the model during injection into or retraction from the tunnel, or during tunnel starts. The sting cross section is elliptical (Fig. 3) to optimize strength and clearance for oscillating slender models.

C. Models

The three models used for the wind tunnel verification tests included an AGARD Calibration Model B, an AGARD Calibration Model C which was made by adding a tail assembly to the Model B (Fig. 4), and the Model B without wings. These models were borrowed from the Cornell Aeronautical Laboratory. The body is a tangent ogive-cylinder (4.5 in. diam) with a fineness ratio of 8.5. The 60° delta wing has a symmetrical circular-arc cross section with a thickness ratio of 0.04 and a span of 4 body diameters. The tail assembly for the Model C consists of a cylindrical body that is 1.5 body diam long on which is mounted a T tail. The horizontal tail is a 60° delta which is located 1.42 body diams above the body centerline, and has a span of 1.63 diams. The vertical tail is swept 60° and tapered to produce a trailing-edge angle of 45°. The cross section of the horizontal and vertical tails is also a symmetrical circular arc with a thickness ratio of 0.04. The model body was constructed of aluminum, with a steel section at the wing mounting location. The wings were aluminum, and the tail assembly for Model C was steel. The model was mounted to the test mechanism so that there were 3.1 body diams from the model base to the sting flare for Model C.

D. Wind Tunnel

Tunnel A is a continuous, closed-circuit, variable-density wind tunnel with an automatically driven flexible-plate-type nozzle and a 40 by 40 in. test section. The tunnel can be operated at Mach numbers from 1.5 to 6 at maximum stagnation pressures from 29 to 200 psia, respectively, and stagnation temperatures up to 750°R ($M_\infty = 6$). Minimum operating pressures range from about one-tenth to one-twentieth of the maximum at each Mach number. Mach number changes may be made without stopping the tunnel in most instances. The model can be injected into the tunnel for a test run and then retracted for model changes without stopping the tunnel flow.

V. Results and Discussion

The results obtained in the bench tests using the two-arm magnetic damper (no model) are presented in Fig. 5. The damping measurement M_q shows excellent agreement with the damper input $M_{q_{\text{mag}}}$, over a large range of magnitudes when the sting is rigid for both balanced and unbalanced test assemblies. The uncertainty in the damper is 2% of the input value. Figure 5 also shows the effect of the sting oscillation, caused by an unbalance, on the damping measurement, and indicates that accurate data can be obtained only if the sting oscillations are included in the data reduction. For the bench tests there were no corrections because of the z movement, which only affects aerodynamic measurements [see Eq. (6)]. The legend in Fig. 5 shows that the natural frequency ω_{n_f} of the model-flexure system can be determined accurately if the sting oscillations are considered (53.92 as compared with 53.45), but is considerably in error if the sting oscillation corrections are omitted (49.72). The model moment of inertia I_y, which was constant for all three unbalanced cases ($Wx_{cg} = 0.233$), would have been calculated erroneously if the sting oscillation corrections had not been applied.

The experimentally measured dynamic and static derivatives obtained in the wind tunnel verification tests for the AGARD calibration Model C at $M_\infty = 2.5$ are presented in Fig. 6 to show the effect of sting oscillations on the data. Omitting the sting oscillations from the data reduction results in measurements which indicate too much dynamic stability and too little static stability. The static stability derivative C_{m_α}, obtained from the slope of the C_m vs α_M measurements, is also presented in Fig. 6, and is in excellent agreement with the oscillatory data which have been corrected for sting oscillations.

The experimentally measured dynamic and static stability derivatives at zero angle of attack are presented in Fig. 7 as a function of Mach number. The dynamic stability of Model C decreases slightly with increasing Mach number, whereas the dynamic stability of Model B and Model B body alone is practically invariant with Mach number. Estimates of $C_{m_q} + C_{m_{\dot{\alpha}}}$ for Model B were obtained from Refs. 4 (wing) and 5 (body), and are in good agreement with the present data. The trend of the static stability derivative C_{m_α}, with Mach number, varies considerably with the model configuration. The largest gradient of C_{m_α}, with M_∞, is obtained with Model C, which changes from stable to unstable at $M_\infty = 2.8$. The data obtained from the slope of C_m vs α_M are presented and are in excellent agreement with the oscillatory data.

VI. Conclusions

Data reduction equations for obtaining pitch or yaw dynamic stability derivatives using both the forced-and free-oscillation techniques were derived from the equations of motion which included sting oscillations. Two methods of obtaining the sting oscillations were presented; viz, measurements using strain gages on the sting with analog electronics, and calculations using the force equation of motion and known static force data. Bench tests using a magnetic damper and wind tunnel tests using AGARD Calibration Model B and Model C verified that accurate data could be obtained if the present data reduction equations were used. Considerable error in the data was shown when the sting oscillations were omitted in the data reduction.

References

[1]Burt, G. E., "A Description of a Pitch/Yaw Dynamic Stability, Forced-Oscillation Test Mechanism for Testing Lifting Configurations," Arnold Engineering Development Center, Arnold AFB, Tenn., AEDC-TR-73-60 (AD762286), June 1973.

[2]Schueler, C. J., Ward, L. K., and Hodapp, A. E., Jr., *Techniques for Measurements of Dynamic Stability Derivatives in Ground Test Facilities*, AGARDograph 121, 1967.

[3]Wittrick, W. H., "The Theory of Symmetrical Crossed Flexure Pivots," SM. 108, Jan. 1948, Council for Scientific and Industrial Research, Dept. of Aeronautics, Melbourne, Aus.

[4]Henderson, A., Jr., "Pitching-Moment Derivatives C_{m_q} and $C_{m_{\dot{\alpha}}}$ at supersonic Speeds for Slender-Delta-Wing and Slender Body Combination and Approximate Solutions for Broad-Delta-Wing and Slender-Body Combination," NACA TN 2553, 1951.

[5]Murphy, C. H. and Schmidt, L. E., "The Effect of Length on the Aerodynamic Characteristics of Bodies of Revolution in Supersonic Flight," Ballistic Research Lab., Aberdeen Proving Ground, Md., Rept. 876, Aug. 1953.